Journal of the Brazilian Society of Mechanical Sciences and Engineering (2020) 42:143
https://doi.org/10.1007/s40430-020-2232-7

TECHNICAL PAPER

Equivalent mechanical model of rectangular container attached to a pendulum compared to experimental data and analytical solution

Marcus V. G. de Morais[1,3] · Alejandro A. O. Lopez[2] · Juliano F. Martins[3] · Lineu J. Pedroso[2]

Received: 8 September 2019 / Accepted: 12 February 2020 / Published online: 20 February 2020

Abstract

A tuned liquid damper (TLD) is a passive control device that transfers kinetic energy from the main structure to a liquid sloshing in a tank. The mechanical description of a sloshing liquid contained in a tank requires an intricate mathematical formulation. An alternative technique describes the TLD dynamic behavior as an equivalent mechanical model comprising a series of pendulums or mass–spring systems attached to the tank walls. To validate this approach, this paper compares the discrete model to experimental results and an analytical solution for a rectangular container attached to a pendulum (pendulum-slosh problem). At first, the fundamental oscillation period of the discrete model, representing a rectangular tank, is compared to experimental data and a classic analytical solution. Finally, we compare the pendulum-slosh problem modeled as a discrete model with the analytical solution and experimental results.

Keywords Sloshing · Continuous model · Discrete equivalent model · Experimental analysis · Video motion capture · Levenberg–Marquardt

1 Introduction

Light and flexible structures have been made possible with advancements in new materials and actual construction systems. When subjected to wind, waves and earthquakes, it is necessary to reduce the dynamic structural response to increase lifetime or comfort criteria. An economical way to control excessive vibration levels is to apply a passive control device, for example, a tuned liquid damper (TLD). A tuned liquid damper consists of a tank partially filled with liquid, usually water, properly tuned to absorber the vibrational excitation energy. Application examples can be found in buildings [1–4], wind turbines [5, 6], bridges [7, 8] and offshore structures [9]. Many tall structures have been effectively fitted with TLD devices, resulting in a significant decrease in structural motion [10, 11].

A TLD is a kind of tuned mass damper that transfers kinetic energy from the main structure to a liquid sloshing in a tank. Although TLD construction is simple, the mechanical description of a sloshing liquid contained in a tank requires an intricate mathematical formulation, as seen in Abramson [12], Dodge [13] and Ibrahim [14].

As an alternative, Dodge [12, 13] described the dynamic responses of sloshing tanks for different geometries as an equivalent mechanical model composed of a sum of mass–spring systems attached to container walls. Dodge [13] summarized the equivalent mechanical model and presented an approach to describe the nonlinear effects and experimental derivation of a parameter model. Li et al. [15] developed a semianalytical/numerical method for equivalent mechanical models of a sloshing fluid in an arbitrarily

Technical Editor: Thiago Ritto.

✉ Marcus V. G. de Morais
mvmorais@unb.br

Alejandro A. O. Lopez
alejandroaugustoospinalopez@gmail.com

Juliano F. Martins
juliano.martins@hotmail.com

Lineu J. Pedroso
lineu@unb.br

[1] Department of Mechanical Engineering, University of Brasília, Darcy Ribeiro Campus, Asa Norte, Brasília, DF 70910-900, Brazil

[2] Department of Civil Engineering, University of Brasília, Darcy Ribeiro Campus, Asa Norte, Brasília, DF 70910-900, Brazil

[3] PPG, Graduate Program in Engineering Material Integrity, University of Brasilia (UnB), Campus of Gama (FGA), Gama (Brasília) 72444-240, Brazil

shaped aqueduct. Only the first sloshing mode is considered for the analytical expressions of the equivalent models and their locations. A supplementary study [16] described an exact solution of an equivalent mechanical model of a sloshing fluid in a rectangular tank. Tait et al. [17, 18] studied additional energy dissipation mechanisms such as damping screens and a sloping bottom. Kareem and Sun [19] presented an analysis of a sloshing fluid subject to stochastic excitation. The concepts of equivalent mass and damping can be used to experimentally determine the estimated values of an equivalent TMD by a shaking table test [20]. An equivalent fluid model is still the preferred choice for structural engineers.

The nonlinear dynamic characteristics of fluid sloshing are observed when external excitations develop high sloshing amplitude (breaking waves) [13, 14]. Yu et al. [21] studied a numerical model of a TLD as an equivalent tuned mass damper with nonlinear stiffness and damping. The model incorporates the stiffness hardening property of the TLD under large amplitude excitation. In addition, semiempirical models of nonlinear TLD behavior were suggested by Sun et al. [22].

Equivalent mechanical models are also described by a series of pendulums to represent the oscillation of a sloshing fluid [13]. Nickawde et al. [23] and Yue [24] modeled the sloshing motion as a simple pendulum to study the stability of a coupled slosh-vehicle system. They employed pendular equivalent mechanical models to carry out studies on the modeling and control dynamics of spacecraft with fuel slosh. Cooker [25] presented a linear analytical approximation of a rectangular container attached to a pendulum, a rectangular container pendulum solution. De Langre [26] revisited Cooker's problem as a one-degree-of-freedom slosh mode.

In this paper, an equivalent mechanical model is compared to experimental results and an analytical solution of a rectangular container sloshing and a coupled pendulum-slosh problem (Cooker's sloshing experiment). The experimental data of the fundamental period are obtained by a simple experimental procedure based on a floating element sensor and motion capture by video. First, the fundamental period of the rectangular tank is compared to the equivalent mechanical model analytical solution and experimental results. The equivalent discrete models could correctly simulate the surface wave's natural period in the tank. Finally, we compare the pendulum-slosh problem modeled as a discrete equivalent model for the coupled system of a rectangular container attached to a pendulum. In this example, we observe better agreement when the equivalent model comprises a series of pendulums.

Using a simplified experimental procedure, the proposed modeling of a coupled pendulum-slosh problem by an equivalent mechanical model was validated by experimental results and analytical solutions. In the literature, experimental investigations [3, 27–35] use intricate and costly techniques with lasers, video capture and/or capacitive wave sensors to acquire wave motion. For an analytical comparison, Love and Tait [34, 35] compared a 2D pendulum-slosh system using an equivalent mechanical technique with experimental results.

In Sect. 2, we present a mathematical description of fluid sloshing in a rectangular reservoir-suspended pendulum. This section presents an analytical solution and the proposed discrete model of Cooker's sloshing experiment. The experimental apparatus and the procedure of modal parameter identification are described in Sect. 3. Finally, in Sect. 4, the discrete equivalent model is compared to the analytical solution and experimental results of Cooker's sloshing experiment.

2 Sloshing in a rectangular tank-suspended pendulum

It is important to differentiate shallow water tanks from deep water tanks. Some authors may model water tanks differently depending on this condition. Le Méhauté [36] defined, for a first approximation of linear theory, that there are three different classifications for describing a standing wave, which are deep water ($H/L > 0.5$), intermediate water depth ($0.5 > H/L > 0.05$) and shallow water ($H/L < 0.05$).

Motivated by the observation of the interaction of the pendulum movement coupled to a tank filled with liquid at different levels and how the walls of the tank generate waves that affect the motion of the pendulum, Cooker [25], based on the assumption of small displacement of the tank, used linearized shallow water equations to model the motion and derive time-periodic solutions for the system whose periods are governed by a transcendental relation.

2.1 Cooker's sloshing experiment

The isolated tank (Fig. 1), as the first system to be analyzed, is defined in an inertial reference frame (x, y), where the horizontal coordinate is x, and $x = 0$ is halfway along the tank when the tank is in the equilibrium position. The y axis is directed vertically upward, and $y = 0$ is the level of water depth. The tank has a length L and a displacement $X(t)$ so that the end walls lie at $x = \pm d + X(t)$, where $d = L/2$.

The empty container has mass m. The contained liquid has mass $M = \rho LHW$, where ρ is the density and W is the container width. The tank is acted upon by two forces. The first is the horizontal tension component in the supports, which together give a restoring force on the tank $(M + m)gX/l$, where g is local gravity acceleration, directed toward $x = 0$.

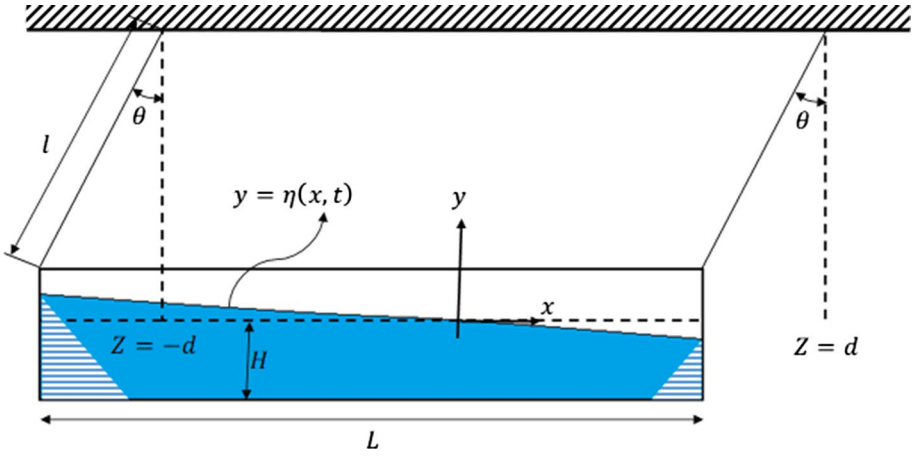

Fig. 1 Schematic representation of a suspended container with sloshing liquid swings like a pendulum [modification of Cooker [25]]

The second force is the wave loading on the end walls, which is approximated by the hydrostatic pressure $\rho g(\eta - y)$ at a position with coordinate $y \leq \eta$. Consequently, if η/H is small, the equation of motion of the pendulum-container system is written as

$$\frac{\mathrm{d}^2X}{\mathrm{d}t^2} = -\Omega^2 + \frac{\rho g W H}{m}[\eta(+d,t) - \eta(-d,t)] \tag{1}$$

where $\Omega^2 = (1 + 1/R)g/l$ and $R = m/M$.

If we apply linearized shallow water theory [12–14], the free-surface displacement $\eta(x,t)$ is calculated by the following expression [25]:

$$\eta(t) = HkX_o \exp(i\omega t)\frac{\sin(kx)}{\cos(kd)} + i\sqrt{H/g}\sum_{n=1}^{\infty}\left[a_n \sin\left(\nu_n t\right)\exp\left(\iota\omega_n t\right) + b_n \sin\left(\mu_n x\right)\exp\left(\iota\sigma_n t\right)\right] \tag{2}$$

where $X_0 = |X|(x = \pm d, t)$ is the absolute horizontal displacement water level at the container walls, H is the container depth, ω is the circular frequency, $k = \omega/\sqrt{gH}$ is the dispersion relation if we assume kH is small, $\nu_n = n\pi/d$, $\omega_n = \nu_n\sqrt{gH}$, $\mu_n = (n - 1/2)\pi/d$, and $\sigma_n = \mu_n\sqrt{gH}$. If the tank is held rigid so that $X_0 = 0$, then usual standing waves occur. The symmetric and antisymmetric free-surface modes have wavenumbers $\nu_n = 2n\pi/L$ and $\mu_n = (2n - 1)\pi/L$, respectively, where n is an integer. The term $n = 1$ gives the fundamental mode with period $T_s = L/\sqrt{gH}$.

Using (2) to describe the surface elevation η, we have the following:

$$\frac{\mathrm{d}^2X}{\mathrm{d}t^2} = -\Omega^2 + \frac{X_o Hkg}{Rd}\tan(kd)\exp(i\omega t) + 2i\frac{\rho W H\sqrt{gH}}{m}\sum_{n=1}^{\infty} b_n(-1)^n \exp\left(i\sigma_n t\right) \tag{3}$$

The temporal solution of Eq. (3) is as follows:

$$X(t) = B\exp(i\omega t) + C\exp(i\Omega t) + \sum_{n=1}^{\infty} D_n \exp\left(i\sigma_n t\right) \tag{4}$$

where C is an arbitrary constant and $R = m/M = m/\rho WHL$.

$$B = \frac{X_o kgH\tan(kd)}{Rd\left(\Omega^2 - \omega^2\right)} \text{ and } D_n = \frac{ib_n\sqrt{gH}(-1)^n}{Rd\left(\Omega^2 - \sigma_n^2\right)} \tag{5}$$

By considering $X(t) = X_0\exp(i\omega t)$ as the periodic solutions of Eq. (3), then we must have $C = 0$ and $D_n = 0$. We arrive at a condition for the wavenumber, for which the periods are governed by roots of the transcendental equation as follows:

$$\frac{G}{s} - Rs = \tan(s) \tag{6}$$

where $s = kd$ and $G = (1 + R)d^2/Hl$.

Equation (6) has an infinite set of positive solutions for s, which in order of increasing size are $s_1, s_2, s_3, \ldots$, where for strictly positive G and R, the roots lie in the interval $0 < s_1 < \pi/2$, and for $n \geq 2, (n - 3/2)\pi < s_n < (n - 1/2)\pi$. Root s_1 corresponds to the longest wavelength, for which the tank and wave motions are in phase.

As shown by the left- and right-hand sides of Eq. (6), $s = kd$ represents the points of intersection of the two curves that give the roots $s_1, s_2, \ldots$ The smallest s_1 corresponds to the fundamental mode.

Root s_2 corresponds to a range of surface shapes with between one and three nodes: If there is one node, then the surface oscillates in antiphase with the tank. The higher modes are less important and correspond to short wavelengths that are not appropriately modeled under the assumption that $kH \ll 1$. The fundamental period T corresponds to $T = \pi L/\left(s\sqrt{Hg}\right)$.

Comparing the coupled period T with the natural period of an empty tank $T_p = 2\pi\sqrt{l/g}$ of length l (moving as a simple pendulum) and the fundamental period of the standing wave $T_s = 2L/\sqrt{Hg}$ (for the tank held fixed), we can conclude as an important general result that when the coupled system oscillates, its period T is greater than T_p and T_s

2.2 Equivalent mechanical models

The dynamic effect of lateral sloshing can be equally well represented by an equivalent (spring–mass) mechanical model. A filled tank may be considered an element of only one mass since the water does not have a free surface to oscillate. When there is a free oscillating surface, the tank can be considered an element with two different masses. The first is called the impulsive mass m_o (rigidly attached to the tank), and the second is called the convective mass m_1 (the oscillating water portion inside the container), as shown in Fig. 2. In Graham and Rodriguez's model [13], m_1 is connected to the tank through stiffness springs $k_1/2$ (when we consider one spring–mass, we consider the fundamental mode of sloshing). Higher modes ($n>1$) have low importance for vibration control. The model parameters such as m_1, k_1, and m_o are determined as a function of the tank shape ratio $f(H/L)$.

The coefficient m_{liq} corresponds to the total liquid mass in the tank, h_0 is the height of the impulsive mass, and h_1 is the height of the convective mass. The fundamental frequency of the container ω_1, considering only the convective mass, is equal to $\omega_1 = \sqrt{k_1/m_1}$ for rectangular tanks with length L and water height H.

Considering bidimensional sloshing modes excited by an imposed x-direction translation of a container, the fluid force amplitudes exerted on the container's lateral surface are expressed as:

$$\frac{F_{x0}}{-\Omega^2 X_0 m_{\text{liq}}} = 1 + 8\frac{L}{H}\sum_{n=1}^{N}\frac{\tanh\left((2n-1)\pi H/L\right)}{(2n-1)^3}\frac{\Omega^2}{\omega_n^2-\Omega^2} \tag{7}$$

where $F_{x0} = F_{x0}^R - F_{x0}^L$, as represented in Fig. 1, is the hydrostatic resultant force. Equation (7) is compared with the following expression for force due to a spring–mass model:

$$\frac{F_{\text{amp}}}{-\Omega^2 X_o m_{\text{liq}}} = 1 + \sum_{n=1}^{N}\frac{m_n}{m_{\text{liq}}}\frac{\Omega^2}{\omega_n^2-\Omega^2} \tag{8}$$

Then, the inertial mass m_n is expressed as

$$m_n = \frac{8}{\pi^3}\frac{L}{H}\frac{\tanh\left((2n-1)\pi H/L\right)}{(2n-1)^3}m_{\text{liq}} \tag{9}$$

The natural frequencies of rectangular containers are

$$\omega_n^2 = (2n-1)\pi(g/L)\tanh\left((2n-1)\pi H/L\right) \tag{10}$$

Then, the equivalent stiffness parameter k_n is calculated as a function of the spring–mass natural frequency ($\omega_n^2 = k_n/m_n$) as follows:

$$k_n = \omega_n^2 m_n = \frac{8}{\pi^2}\frac{g}{H}\frac{\tanh^2\left((2n-1)\pi H/L\right)}{(2n-1)^2}m_{\text{liq}} \tag{11}$$

According to the continuity equation $m_0 + \sum m_n = m_{\text{liq}}$, impulsive mass m_o is calculated by:

$$m_0 = \left[1 - \frac{8}{\pi^3}\frac{L}{H}\sum_{n=1}^{N}\frac{\tanh\left((2n-1)\pi H/L\right)}{(2n-1)^3}\right]m_{\text{liq}} \tag{12}$$

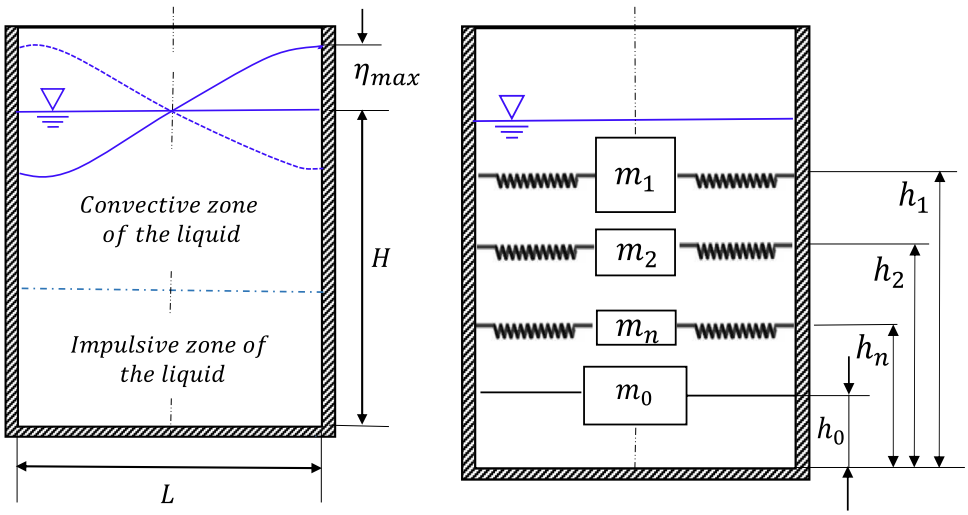

Fig. 2 Lateral sloshing in a rectangular container (**a**) described as an equivalent mechanical model composed of an additional inertial mass m_o and inertial masses $m_i (i = 1 \ldots n)$ coupled to spring dashpots $k_i (i = 1 \ldots n)$ (**b**)

2.2.1 Proposed equivalent model for Cooker's pendulum

Cooker's pendulum (Fig. 1) can be described as an equivalent spring–mass mechanical system coupled to a pendulum. Figure 3 models the container's sloshing liquid as only one equivalent spring–mass system to describe the fundamental sloshing mode ($n = 1$).

The equation of motion for the pendulum, representing the main system reduced to a degree of freedom, is presented as a matrix as follows:

$$\begin{bmatrix} (m+m_{\text{liq}})l^2 & m_1 l \\ m_1 l & m_1 \end{bmatrix} \begin{Bmatrix} \ddot{\theta} \\ \ddot{x}_1 \end{Bmatrix} + \begin{bmatrix} (m+m_{\text{liq}})gl & 0 \\ 0 & k_1 \end{bmatrix} \begin{Bmatrix} \theta \\ x_1 \end{Bmatrix} = \begin{Bmatrix} 0 \\ 0 \end{Bmatrix} \tag{13}$$

3 Experimental procedure

In this section, we briefly describe the experimental procedure used to identify the sloshing oscillation frequency of a rectangular container (filled with water) put over a pendulum. In Sect. 3.1, a description of the experimental apparatus presents how the dynamic level of the liquid free surface was measured. In Sect. 3.2, temporal responses are fitted using a damped harmonic function to characterize the experimental modal parameters. The Levenberg–Marquardt nonlinear least-squares technique in the Curve Fitting Toolbox/MATLAB was used to fit the time responses of the free surface. The determination of the experimental modal parameters of natural frequency and damping ratio as a function of the fitted coefficients was carried out using a damped harmonic function, as described in Sect. 3.2.

3.1 Description of experimental apparatus

To accomplish the free surface experimental setup, a liquid volume is contained in a rectangular reservoir (glass aquarium) relative to various liquid depths. The dimensions of the reservoir are width $L = 294$ mm, depth $W = 150$ mm and height $H = 196$ mm (max). The mass of the empty reservoir is $M_r = 808$ g. In the laboratory of vibration and dynamic metrology (latitude −15.7633°, longitude −47.8731° and altitude 1020 m), in Brasilia, Brazil, the local gravity acceleration is $g = 9.7808$ m/s^2 (measured by a LaCoste & Romberg gravity meter, model G no. 613). In addition, in these experiments, the liquid was potable water with density $\rho \simeq 997$ kg/m^3.

The free surface movement was captured using a digital camera (of a Galaxy S3 cell phone) at 30 frames per second (fps) and the motion capture shareware program CvMob [37]. To address the difficulty in capturing the free surface level due to the fluid meniscus, a floating element (fishing buoy) was used as a tracker. The buoy travels vertically along a nylon wire suspended from the bottom and upper sides of the reservoir. Figure 4 presents a schematic representation of the floating element disposition to experimentally track (using a digital camera and a motion capture program) the liquid's dynamic level at a specific point on the free surface of a rectangular reservoir. Figure 5 shows an example of the liquid's dynamic level by motion capture using CvMob and the digital video camera. At the left, we observe the motion capture of the floating element represented by green points. At the right, the horizontal motion of the floating element is plotted against time.

Modeled as a mass–spring, the floating element is described by the dynamic equation $\ddot{u} + \omega_{nb}^2 u = \omega_{nb}^2 \eta$, where the buoy's oscillation natural frequency is $\omega_{nb}^2 = \rho g \pi R_b^2 / m_b$, the floating element rayon $R_b = 5.5$ mm, and the floating element mass $m_b = 0.20$ g. The floating element's estimated natural frequency is $\omega_{nb} = 68$ rad/s, which is several times superior as the higher frequency ($< 2\pi$rad/s). Supposing that the free surface follows a harmonic function (e.g., $\eta(t) = \eta_o \sin \Omega t$), the

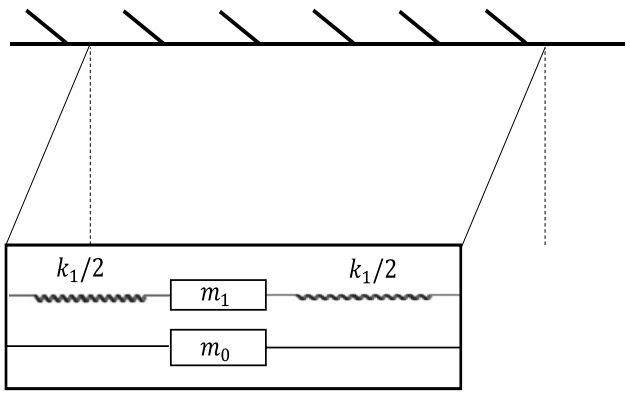

Fig. 3 Lateral pendulum coupled to an impulsive mass m_o and one spring–mass (k_1, m_1) equivalent model

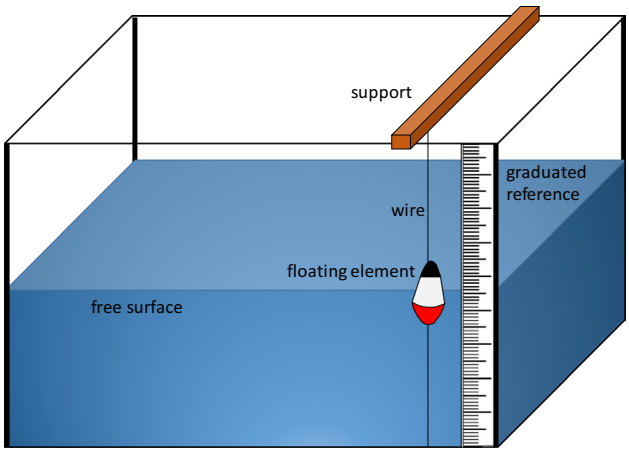

Fig. 4 Schematic of the floating element disposition to track the liquid dynamic level at a specific point on the free surface of the rectangular reservoir

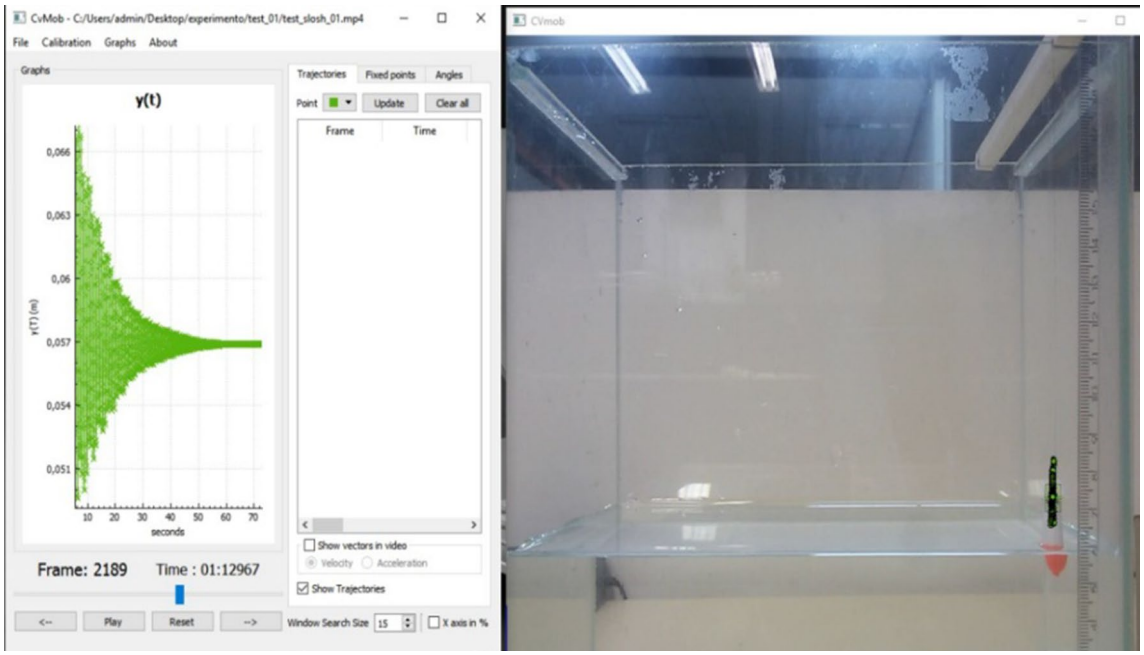

Fig. 5 Example of the liquid's dynamic level by motion capture software CvMob

ratio between the float movement and free surface is near unity ($u/\eta \sim 1$) for this experiment's frequency range, in which the dynamic response of the floating element is not amplified, generating measurement error.

3.2 Identification of modal parameters

The Curve Fitting Toolbox (CFTOOL/MATLAB) was used to carry out the adjustment of a damped harmonic motion function $g(x) = a_1 \exp\left(-a_2 t\right) \sin\left(a_3 t + a_4\right) + a_5$ compared to an experimental trajectory obtained by the motion capture software CvMob. The Levenberg–Marquardt residual sum minimization method was chosen.

For the adjustment of experimental data, the fitting function (written as a damped harmonic motion) is described as follows:

$$g(t) = A \exp\left(-\xi\omega_n t\right) \sin\left(\omega_d t + \phi\right) + B \tag{14}$$

In this case, function $g(t)$ is a function with five adjustment parameters: $a_1 = A$, $a_2 = \xi\omega_n$, $a_3 = \omega_d$, $a_4 = \phi$, and $a_5 = B$, where A is the amplitude constant, $\xi\omega_n$ is the product of the viscous damping coefficient ξ and natural frequency ω_n, ω_d is the damped frequency, ϕ is the phase angle, and B is the experimental offset due to the definition of the origin. For the nonlinear adjustment, we look for minimization of nonlinear temporal functions $g\left(t, a_1, a_2, \ldots, a_5\right)$ used to adjust the signal dataset $\left[y_1, y_2, \ldots, y_m\right]$, where $m \gg 5$. Appendix A: Curve Fitting Toolbox shows an example of the identification of modal parameters obtained by capture of the liquid's dynamic level, as shown in Fig. 5.

Therefore, to obtain the parameters $a_i (i = 1, \ldots, 5)$ that minimize Eq. (14), which approximates the trajectories of the float, for each level that the tank is filled, we proceed to obtain the studied parameters, experimental natural frequency $\left(\omega_n\right)_{\text{exp}}$ and experimental damped frequency $\left(\omega_d\right)_{\text{exp}}$. The damped frequency ω_d is a function of the damping ratio ξ and natural frequency ω_n of a dynamic system as follows:

$$\omega_d = \omega_n \sqrt{1 - \xi^2} \tag{15}$$

By algebraic manipulation, we can transform Eq. (15) as a function of the experimental parameters as follows:

$$\left(\omega_n\right)_{\text{exp}}^2 = \left(\omega_d\right)_{\text{exp}}^2 + \left(\omega_n \xi\right)_{\text{exp}}^2 \tag{16}$$

where $\left(\omega_d\right)_{\text{exp}}$ and $\left(\xi\omega_n\right)_{\text{exp}}$ are provided by functions for damped harmonic vibration that best fit the experimental trajectories. By this procedure, the modal parameters of natural frequency $\left(\omega_n\right)_{\text{exp}}$ and damping ratio $(\xi)_{\text{exp}}$ can be estimated with reasonable precision.

4 Results and discussion

In this section, we carry out the modal parameter identification of (a) rectangular container slosh motion and (b) coupled slosh motion and a suspended rectangular container (Cooker's sloshing experiment) [25, 38]. The obtained experimental results (by the presented experimental

methodology) are compared with the analytical solution and mechanical equivalent model.

4.1 Validation by rectangular container slosh motion

The free surface of the rectangular container partially filled with water was examined to validate the experimental procedure. After the reservoir is subjected to a perturbance (an impulse), the float element is filmed for more than 20 periods of oscillation to determine the free surface's dynamic behavior. This approach seeks to experimentally identify the first sloshing oscillation period for different liquid heights.

Figure 6 compares the experimental sloshing period $T(s)$ as a function of the aspect ratio H/L compared to the analytical solution (10) and discrete model solution. The results present good agreement with the analytical solution. As expected, the solution based on the equivalent mechanical model is identical to the analytical solution. The relative error between the analytical solution and equivalent model was less than 2%.

Figure 7 compares the slosh period of oscillation $T(s)$ as a function of the aspect ratio H/L to different water wave theories (shallow and deep waters). The uncertainty envelope corresponds to the combined standard uncertainty [39], where the sensitivity coefficients are determined from the analytical solution (10). The experimental results for the slosh period of oscillation in the rectangular container are preponderantly characterized in shallow and intermediate water.

However, the reduction in the movement of the liquid by an equivalent system composed of only one mass–spring or pendulum can be a very strong approximation. In the comparison, there is good agreement between the model pendulum structure, a sloshing pendulum, in the experimental results and the analytical solution for the coupled system. The equivalent model of the sloshing pendulum manages to achieve a greater approximation. Figure 8 shows an analysis of convergence for the higher modes; the equivalent pendulum model presents a faster convergence for the first two convective masses.

4.2 Validation of Cooker's sloshing experiment

The present study consists of Cooker's sloshing experiment using the rectangular tank placed on a pendular platform (base supported by inextensible wires). The pendular platform has different lengths $L = [290;407;537]$ mm and a pendulum mass $M_p = 2454.0$ g. The experimental study performs free vibration analysis of Cooker's pendulum using video motion capture. The experiments are carried out for an initial displacement of 106 mm for several water levels (variable aspect ratio). The pendulum motion is video recorded by a digital camera and captured using CvMob software. Each experiment is repeated three times.

Figure 9 shows the evolution of the experimental fundamental period of oscillation of Cooker's sloshing experiment as a function of the aspect ratio for different pendulum lengths L. The analytical coupled solution (6) (continuous line) and equivalent mass model (13) (dotted line) (discretized with 10 mass–spring models) show reasonable agreement with the experimental results. The present experimental results support the hypothesis of $kH < 1$.

Figure 10 shows the experimental damping ratio $\xi[\%]$ results as a function of the aspect ratio for different pendulum lengths l. These results are necessary to determine the optimum parameters for passive control applications [40].

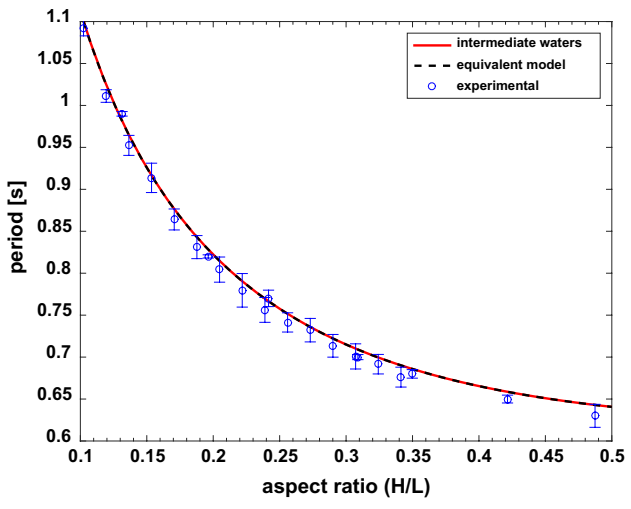

Fig. 6 Sloshing period $T(s)$ versus aspect ratio H/L. Comparison of experimental results (o) by report to analytical solution (10) (solid line) and equivalent mechanical model (—)

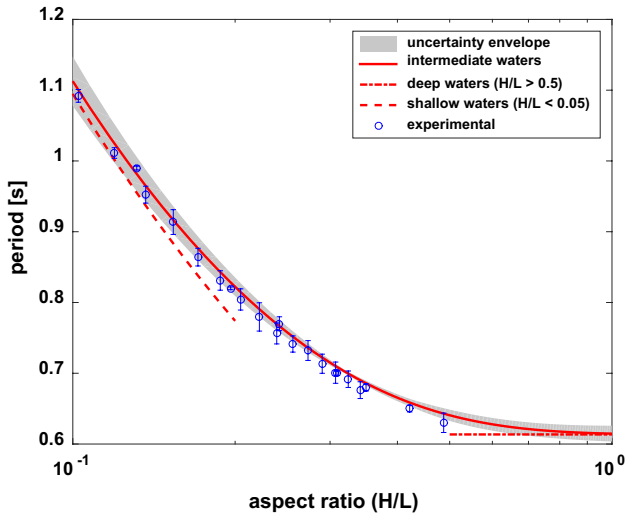

Fig. 7 Comparison of experimental sloshing period $T(s)$ versus aspect ratio H/L by report to different solutions. The uncertainty envelope (gray shading) corresponds to the combined standard uncertainty

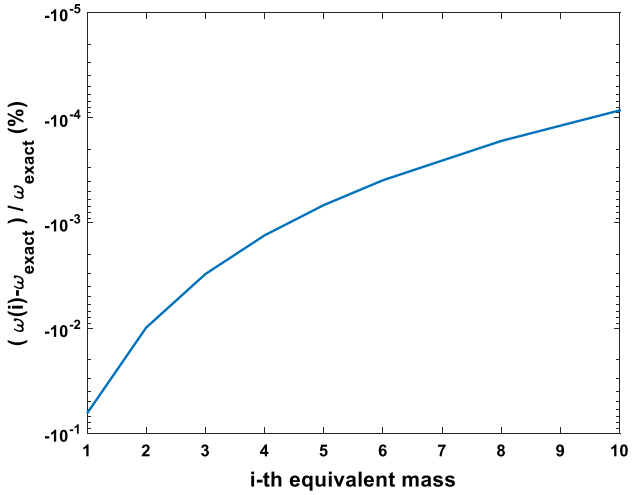

Fig. 8 Convergence of the oscillation frequency ω_i[rad/s] of the discrete model as a function of the i(th) equivalent mass. The ordinate presents the relative error $(\omega_i - \omega_{\text{exact}})/\omega_{\text{exact}}(\%)$

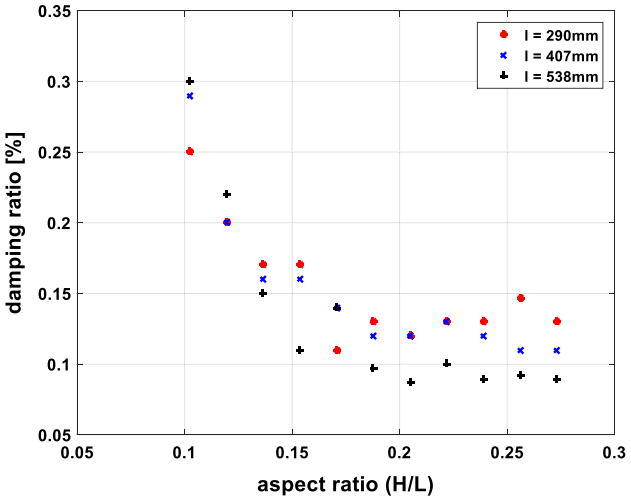

Fig. 10 Experimental damping ratio $\xi[\%]$ as a function of the aspect ratio H/L for different pendulum lengths l ("·"$l = 290$ mm, "×"–$l = 407$ mm, "+"–$l = 538$ mm)

The damping ratio is less influenced by the pendulum length l, contrarily observed in oscillatory period T (Fig. 9).

5 Conclusions

The present work presents a description of sloshing problems by equivalent mass parameters. By comparison with experimental results and a classic solution for a rectangular tank uncoupled (first case) and coupled to a pendulum (second case), equivalent discrete models are validated for the results of the fundamental period of oscillation as a function of the aspect ratio H/L, where H is the liquid depth and L is the reservoir length.

In the first case study, a rectangular tank is modeled by an equivalent mass model. The fundamental oscillation period of the equivalent mass model is compared to experimental data and the classic analytical solution with reasonable agreement.

The last case study shows the fundamental oscillation period of a pendular system suspending a rectangular tank. The dynamic system is modeled as an equivalent model with a spring–mass. The numerical results are compared with respect to experimental results and the coupled analytical solution by Cooker (1994). A reasonable agreement for the results is found by equivalent parameters with respect to the experiments and the analytical solution coupled with relative errors of approximately 10%. This difference can be explained by the approximation of the liquid system by a single equivalent mass–spring system. Complementary studies and new experimental results are required to verify this deviation.

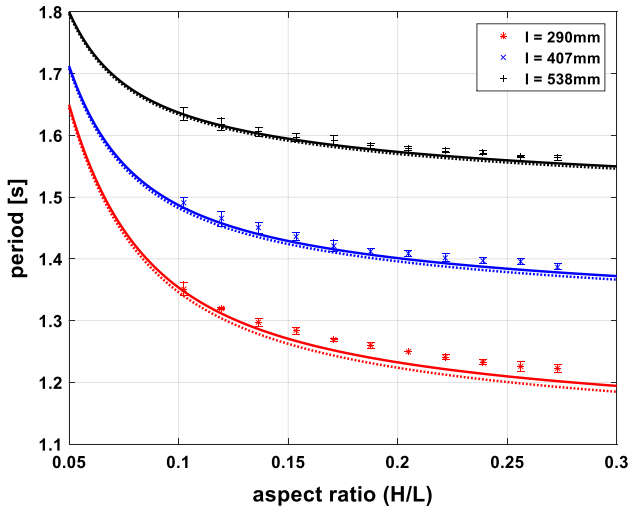

Fig. 9 Experimental oscillation period $T[s]$ as a function of the aspect ratio H/L for different pendulum lengths l ("·"$l = 290$ mm, "×"–$l = 407$ mm, "+"–$l = 538$ mm). Cooker's pendulum analytical solution (continuous line) and mass equivalent model (dotted line) are compared with the experimental data

Acknowledgments This work was supported by the Brazilian Coordination for the Improvement of Higher Education Personnel (CAPES) – Finance Code 001, Brazilian Council for Scientific and Technological Development (CNPq) and Research Support Foundation of the Federal District (FAPDF). The second author acknowledges the Group of Dynamics of Systems (UnB-FT/EnM/GDS) for its support to make possible the present experiments.

Appendix A: Curve Fitting Toolbox

Figure 11 shows an example of dynamic parameter identification performed by the Curve Fitting Toolbox (CFTOOL/MATLAB). This illustration presents the liquid's dynamic

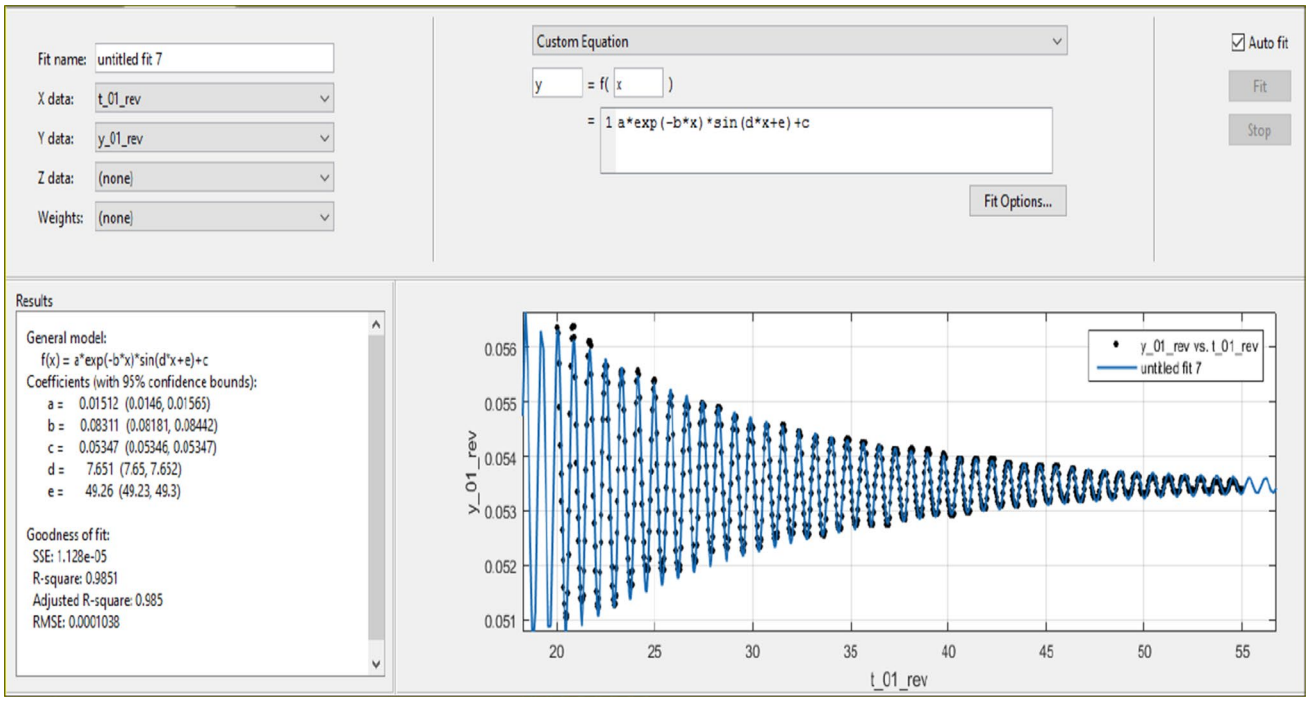

Fig. 11 Example of identification of modal parameters by the Curve Fitting Toolbox (MATLAB)

level motion in a rectangular container observed by motion capture, as shown in Fig. 5.

References

1. Novo T, Varum H, Teixeira-Dias F, Rodrigues H, Silva MF, Costa AC et al (2014) Tuned liquid dampers simulation for earthquake response control of buildings. Bull Earthq Eng 12:1007–1024. https://doi.org/10.1007/s10518-013-9528-2
2. Espinoza G, Carrilloa C, Suazoa A (2018) Analysis of a tuned liquid column damper in non-linear structures subjected to seismic excitations. Lat Am J Solids Struct. https://doi.org/10.1590/1679-78254845
3. Battaglia L, Cruchaga M, Storti M, D'Elía J, Núñez Aedo J, Reinoso R (2018) Numerical modelling of 3D sloshing experiments in rectangular tanks. Appl Math Model 59:357–378
4. Castillo EF, Cruchaga MA (2012) Experimental vibration analysis for a 3D scaled model of a three-floor steel structure. Lat Am J Solids Struct Associação Brasileira de Ciências Mecânicas. 9:597–613
5. Zhang Z, Staino A, Basu B, Nielsen SRK (2016) Performance evaluation of full-scale tuned liquid dampers (TLDs) for vibration control of large wind turbines using real-time hybrid testing. Eng Struct 126:417–431
6. Zhang Z, Nielsen SRK, Basu B, Li J (2015) Nonlinear modeling of tuned liquid dampers (TLDs) in rotating wind turbine blades for damping edgewise vibrations. J Fluids Struct 59:252–269
7. Xue SD, Ko JM, Xu YL (1999) Experimental study on performance of tuned liquid column damper in suppressing pitching vibration of structures. J Intell Mater Syst Struct 10:386–396. https://doi.org/10.1177/1045389x9901000504
8. Shum KM, Xu YL, Guo WH (2008) Wind-induced vibration control of long span cable-stayed bridges using multiple pressurized tuned liquid column dampers. J Wind Eng Ind Aerodyn 96:166–192
9. Lackner MA, Rotea MA (2011) Passive structural control of offshore wind turbines. Wind Energy 14:373–388
10. Noji T, Yoshida H, Tatsumi E, Kosaka H, Hagiuda H (1988) Study on vibration control damper utilizing sloshing of water. J Wind Eng. 37:557–566
11. Fujino Y, Pacheco BM, Chaiseri P, Sun LM (1988) Parametric studies on tuned liquid damper (TLD) using circular containers by free-oscillation experiments. Doboku Gakkai Ronbunshu. 1988:177–187
12. Abramson HN (1966) The dynamic behavior of liquids in moving containers with applications to space vehicle technology. Technical Report NASA SP-106, p 467
13. Dodge FT (2000) The new "dynamic behaviour of liquids in moving containers". Technical Report, Southwest Research Institute, San Antonio, TX
14. Ibrahim RA (2014) Recent advances in vibro-impact dynamics and collision of ocean vessels. J Sound Vib 333:5900–5916
15. Li Y, Di Q, Gong Y (2012) Equivalent mechanical models of sloshing fluid in arbitrary-section aqueducts. Earthq Eng Struct Dyn. 41:1069–1087
16. Li Y, Wang J (2012) A supplementary, exact solution of an equivalent mechanical model for a sloshing fluid in a rectangular tank. J Fluids Struct 31:147–151
17. Tait MJ, El Damatty AA, Isyumov N (2002) The dynamic properties of a tuned liquid damper using an equivalent amplitude dependent tuned mass damper. In: 4th Structure Specification Conference on Canadian Society Civil Engineering, p 1–10
18. Tait MJ, Isyumov N, El Damatty AA (2008) Performance of tuned liquid dampers. J Eng Mech Am Soc Civ Eng 134:417–427

19. Kareem A, Sun WJ (1987) Stochastic response of structures with fluid-containing appendages. J Sound Vib 119:389–408
20. Ashasi-Sorkhabi A, Malekghasemi H, Ghaemmaghami A, Mercan O (2017) Experimental investigations of tuned liquid damper-structure interactions in resonance considering multiple parameters. J Sound Vib 388:141–153
21. Yu J, Wakahara T, Reed DA (1999) A non-linear numerical model of the tuned liquid damper. Earthq Eng Struct Dyn 28:671–686
22. Sun LM, Fujino Y, Chaiseri P, Pacheco BM (1995) The properties of tuned liquid dampers using a TMD analogy. Earthq Eng Struct Dyn. 24:967–976. https://doi.org/10.1002/eqe.4290240704
23. Nichkawde C, Harish PM, Ananthkrishnan N (2004) Stability analysis of a multibody system model for coupled slosh-vehicle dynamics. J Sound Vib 275:1069–1083
24. Yue B-Z (2011) Study on the chaotic dynamics in attitude maneuver of liquid-filled flexible spacecraft. AIAA J 49:2090–2099. https://doi.org/10.2514/1.j050144
25. Cooker MJ (1994) Water waves in a suspended container. Wave Motion 20:385–395
26. De Langre E (2001) Fluides et solides. Editions Ecole Polytechnique
27. Park J, Im S, Sung HJ, Park JS (2015) PIV measurements of flow around an arbitrarily moving free surface. Exp Fluids 56(3):56
28. Di Matteo A, Lo Iacono F, Navarra G, Pirrotta A (2015) Innovative modeling of Tuned Liquid Column Damper motion. Commun Nonlinear Sci Numer Simul 23:229–244
29. Di Matteo A, Lo Iacono F, Navarra G, Pirrotta A (2014) Direct evaluation of the equivalent linear damping for TLCD systems in random vibration for pre-design purposes. Int J Non Linear Mech 63:19–30
30. Di Matteo A, Lo Iacono F, Navarra G, Pirrotta A (2014) Experimental validation of a direct pre-design formula for TLCD. Eng Struct 75:528–538
31. Furtmüller T, Di Matteo A, Adam C, Pirrotta A (2019) Base-isolated structure equipped with tuned liquid column damper: an experimental study. Mech Syst Signal Process 116:816–831
32. Di Matteo A, Di Paola M, Pirrotta A (2016) Innovative modeling of tuned liquid column damper controlled structures. Smart Struct Syst. 18:117–138
33. Love J, Tait M (2015) The response of structures equipped with tuned liquid dampers of complex geometry. J Vib Control 21:1171–1187. https://doi.org/10.1177/1077546313495074
34. Love JS, Tait MJ (2013) Equivalent mechanical model for tuned liquid damper of complex tank geometry coupled to a 2D structure. Struct Control Heal Monit 21:43–60
35. Love JS, Tait MJ (2011) Equivalent linearized mechanical model for tuned liquid dampers of arbitrary tank shape. J Fluids Eng 133:61105–61109. https://doi.org/10.1115/1.4004080
36. Le Mehaute B (2013) An introduction to hydrodynamics and water waves. Springer, Berlinm
37. Peña N, Credidio BC, Corrêa LPNRM, França LGS, Cunha M, de Sousa MC et al (2013) Free instrument for measurements of motion. Rev Bras Ensino Física 35:1–5
38. Alemi Ardakani H, Bridges TJ, Turner MR (2012) Resonance in a model for Cooker's sloshing experiment. Eur J Mech B/Fluids. 36:25–38
39. JCGM (2008) Evaluation of measurement data: guide to the expression of uncertainty in measurement. Int Organ Stand 100(1):134
40. Alkmim MH, Fabro AT, de Morais MVG (2018) Optimization of a tuned liquid column damper subject to an arbitrary stochastic wind. J Braz Soc Mech Sci Eng 40:1–11. https://doi.org/10.1007/s40430-018-1471-3